U.V. Derivative spectra studies of some Schiff's Bases of Amino Acids complexes- Trace Amount Determintion.

Isam J. AL- Nuri Amel G. Abed Thana Y. Yousif

College of Science, Mosul University

(NJC)

(Recevied on 15/12/2010) (Accepted for publication 10/ 7/2011)

Abstract

According to the biological and industrial importance of Schiff bases derived from amino acids, the U.V. derivative spectra were studied for Schiff bases derived from Leucine amino acid and their complexes with Ni (II) and Co (II) in ethanol as solvent. The plot of the molar concentration versus the absorbance result in a straight line relationships obeys the Beer's Lambert law with in certain ranges of concentrations. The Zero, first and second order derivative spectra were recorded and the integrated area under the peaks estimated for a solutions of different concentrations which employed for quantification of the complexes of these Schiff bases and shows a relative enhancement in the determination limits as compared with Zero- order technique.

الخلاصة

نظراً للأهمية البايولوجية والصناعية لمركبات قواعد شيف المشتقة من الحوامض الامينية ومعقداتها فقد تمت دراسة أطياف المشتقة لقواعد شيف مشتقة من الحامض الأميني ليوسين ومعقداتها مع النيكل والكوبلت في مذيب الايثانول وتم رسم العلاقة البيانية بين التركيز والامتصاص لعدد من المحاليل مختلفة التركيز وكانت النتيجة خطاً مستقيماً يتطابق مع قانون بير- لامبرت ضمن مديات تركيز معينة. كما تم دراسة اطياف المشتقة الأولى والثانية لمعقدات هذه القواعد وايجاد مديات تقدير التركيز من العلاقة الخطية بين المساحة تحت الحزم المختارة لغرض التقدير والتركيز المولاري لعدد من المحاليل ووجد انه حصل تحسن نسبي في مديات التقدير مقارنة مع طيف المشتقة صفر.

Introduction

Schiff bases and their complexes have received renewed attension in recent years because of their antitumor and carcino static activities. [1, 2]

They are known to exhibit awide variety of pharmacological properties such as antiflammatory,[3] antimalarial[4], antifungal[5] and antiviral. The Schiff bases complexes have numerous industrial applications as oxidant reagents for sulphur compounds[6]. The mixture of Schiff bases with transition metals were used as stablizers in gasoline and polymers.[7] A large number of research works have been acomplished about the complexes of Schiff bases with several metal ions (transition and non- transition), from which the complexes of Co(II), Cu(II) with Schiff bases derived from isatin, glycine and alanine[8], The complexes of Zn(II), Cu(II), Ni(II) with Schiff bases derived from the condensation of 2-hydroxy-1-naphthaldehyde with amino acids L-alanin and L- isoleucine[9]. Many methods for the determination of Schiff bases complexe were established, from these methods. The differential pluse polarographic studies of BenziL-Glycine Schiff base and its Ni (II) complexes in aqueous and DMSO medium[10]. Spectrophtometric method for determination and kinetics of amino acids through their reaction with syringaldehyde.[11] spectrophotometric determination of metronidazole through Schiff's base system using vanillin and PDAB (p-dimethyl amino benzaldehyde) reagents in pharmaceutical preparations.[12] HPLC determination of Schiff bases[13]. Flow injection spectrophotometric determination of Fluoxetine in bulk and in pharmaceutical preparations[14]. Direct determination of Zirconium and chromium complexes with Schiff's base 2-(2-pyridylmethyleneamino) phenol by first- order derivative spectrophotometry.[15] simultaneous determination of Zinc (II) and Nickel (II) with 2-(2-pyridylmethylene amino) phenol by first derivative spectrophotometry. [16] In this work the first and second- order derivative were studied for the complexes of new Schiff bases derived from Leucine amino acid with sodium -3-acetylpyridine (NaL_1) and sodium acetoacetanilide ($NaHL_2$) with Co and Ni and their direct determination.

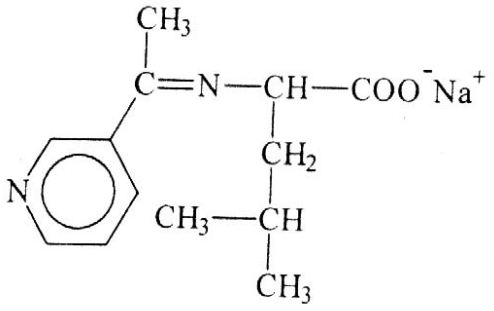

NaL_1

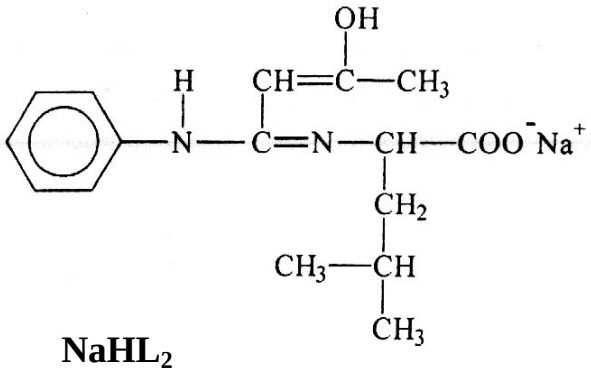

$NaHL_2$

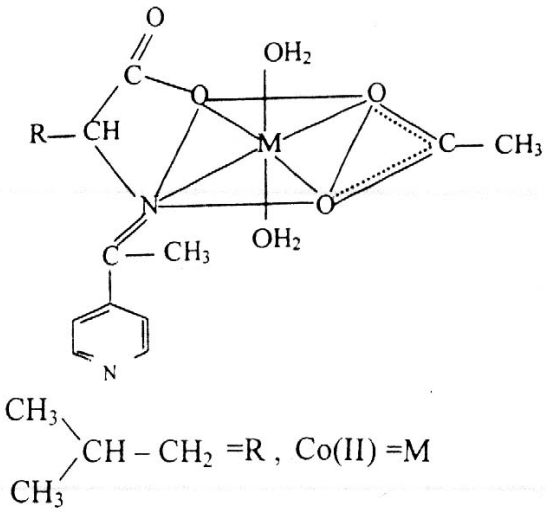

CH_3 – $CH(CH_3)$ – CH_2 =R , Co(II) =M

L_1Co

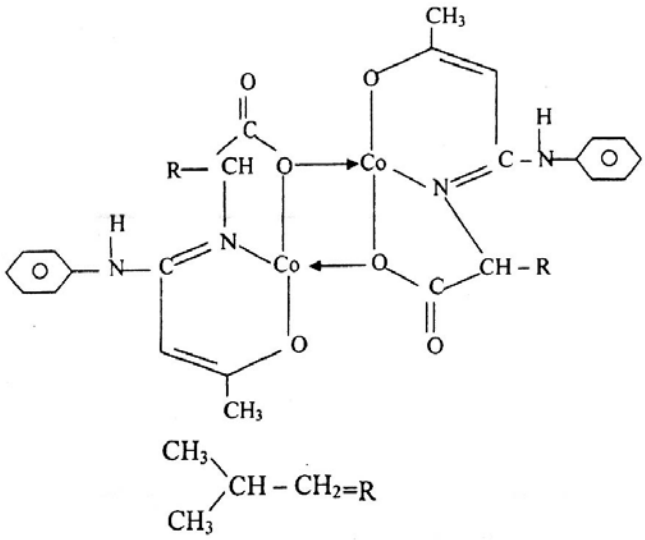

CH_3 – $CH(CH_3)$ – CH_2=R

L_2Co

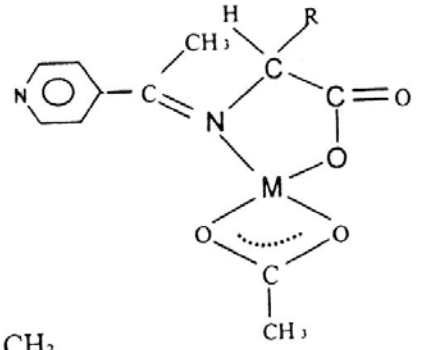

CH_3 – $CH(CH_3)$ – CH_2 =R, Ni(II) =M

L_1Ni

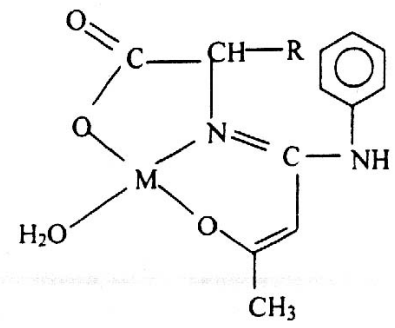

CH_3 – $CH(CH_3)$ – CH_2=R, Ni(II) = M

L_2Ni

Experimental

Chemicals:

All the chemicals and the solvents are of high purity and supplied by Fluka and BDH.

Preparation of Schiff bases salts: [17]

For the preparation of the Schiff base 1-sodium-3-acetylpyridine Leucineimine (NaL_1) with empirical formula $C_{13}H_{17}N_2O_2Na$, mix equimolar amounts [0.01 mole, 1.31gm] of amino acid Leucine with [0.01 mole, 1.21gm] of 3-acetylpyridine in 20 ml 50% ethanol in the presence of sodium acetate 0.01 mole (0.82 gm), heat the mixture to 50°C and reflux at this temperature for 20 min. Cool, Leave the mixture. Measure the pH of the mixture which must be (pH= 5.0-6.6)[18], then evaporate until 1/4 the original volume of the mixture, followed by the addition of 10 ml ethanol until the formation of precipitate, Leave it over night for complete precipitation, filter the precipitate and wash it several times with 5ml, ethanol, then dry under reduced pressure. By the same method the ligand $NaHL_2$ (sodium Acetoacetanilide leucine amine) with empirical formula $C_{16}H_{21}O_3N_2Na$ using Acetoacetanilide (0.01 mole, 1.77gm) was prepared.

Complex preparation[17]:

For the preparation of Co (II) complex of Schiff base sodium 3-acetyl pyridine Lencine imine (L_1Co) with empirical formula $[Co(L_1)(CH_3COO)(H_2O)_2]$, mix equimolar amounts of Leucine amino acid (0.01 mole, 1.31 gm) with 3-acetylpyridine (0.01 mole, 1.21gm) in 20 ml 50% ethanol in the presence of (0.01 mole, 2.49 gm) $Co(CH_3COO)_2$. 4H2O, reflux for 2hrs at 50 °C. Cool at room temperature, check the pH of the mixture, then evaporate to 1/4 of its volume and add 20 ml ethanol, Leave the mixture over night pink color precipitate was separated which filtered and washed with ethanol followed by petroleum ether and dried under reduced pressure. In the same methods the complexes L_1 Ni with empirical formula $[Ni(L_1)(CH_3COO)(H_2O)]$, L_2Co with empirical formula $[Co_2(L_2)_2]$. $2H_2O$ and L_2Ni with empirical formula $[Ni(L_2)(H_2O)]$ were prepared.

Instrumentation:

All the U.V. spectra were recorded using UV- visible spectrophotometer. ShimadZu UV-1650 PC using 1x1x3 Cm matched quartz cells.

For UV-Spectra measurement 25 ml 10^{-2} M solutions in ethanol were prepared by dissolving 0.064 g, 0.0967 g, 0.087 g from NaL_1, L_1Co, L_1Ni

respectively and 0.0789 g, 0.17349, 0.0911 g from NaH L_2, L_2 Co, L_2Ni respectively and by appropriate dilution the solutions 10^{-3} M, 10^{-4} M and 10^{-5} M in ethanol were prepared.

Calculations:

The peak area measurements are often found to be more reliable than peak height measurements, for this reason the quantifications were accomplished according to the integrated area under the peaks under consideration.

Results and Discussion

The U.V. absorption spectra of the Schiff bases NaL_1 and $NaHL_2$ were recorded before the complexation with the metals (Co (II) and Ni (II)) and shows absorption maximum at 264 nm and 240 nm respectively. After their complex formation with metals Co (II) and Ni (II), the U.V. absorption spectra were recorded for a series of solutions at different ranges of concentrations.

Co-Complexes:

The zero-order spectra of the complex L_1Co show an absorption band at λ=238 nm with ε_{max} = 2165 Lit.mole^{-1}.cm^{-1} and another band at λ=276nm with ε_{max}=1315 Lit.mole^{-1}.cm^{-1}, where as the complex L_2Co show absorption band at λ=238nm and 278nm with ε_{max} = 3237 and 3270 Lit.mole^{-1}.cm^{-1} respectively Fig.(1) and (2).

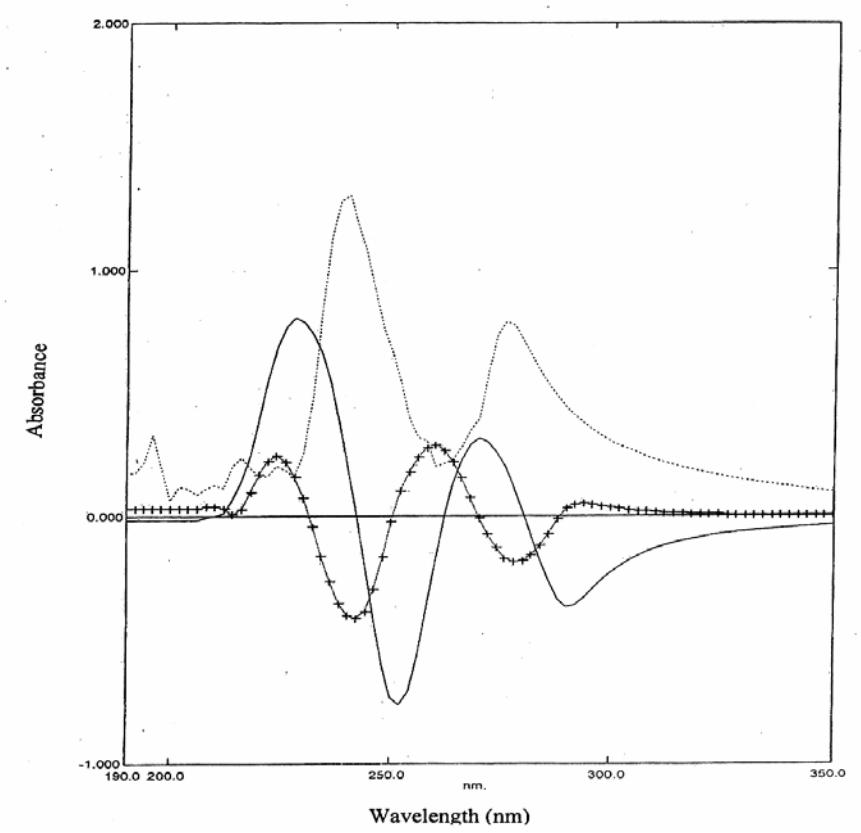

Fig. (1): U.V. absorption spectra of L_1Co complex solution in ethanol. (…. Zero-order, —— first order derivative , ++++ second order derivative).

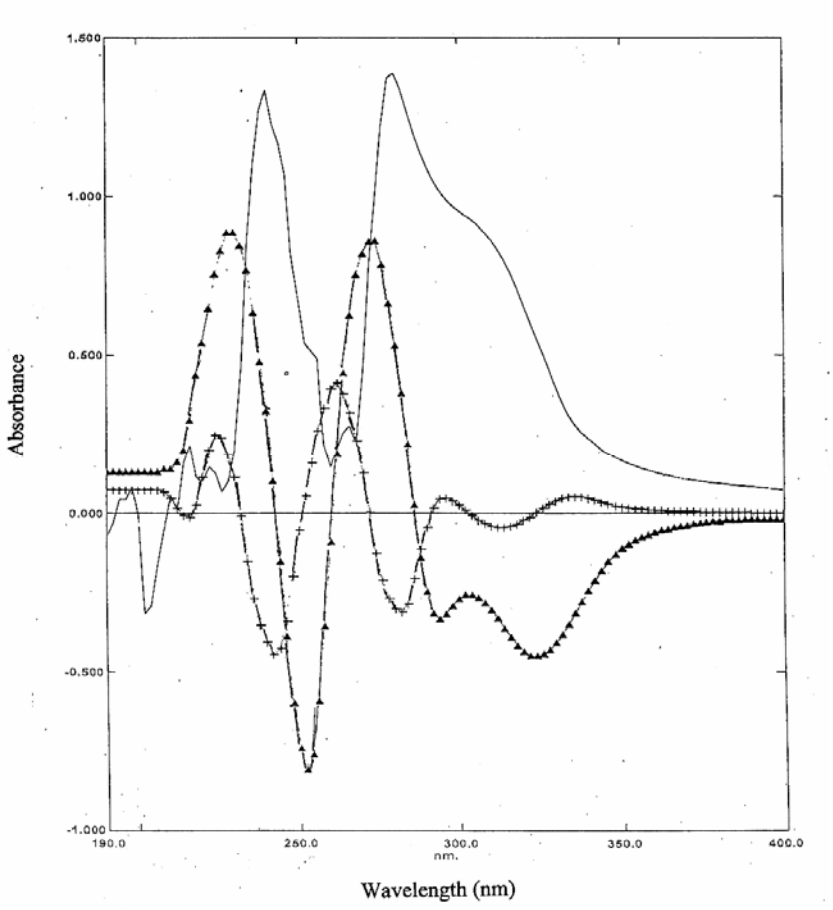

Fig. (2): U.V. absorption spectra of L_2Co complex solution in ethanol. (—— Zero-order, ◄◄◄ first order derivative , +++ second order derivative).

The quantification of the complexes L_1Co and L_2Co were accomplished according to the bands at λ = 276 nm, λ = 278nm respectively through the absorbance measurement for a series of solutions at different concentrations in ethanol and the results are shown in table (1) and (2).

Table (1): The absorbance of different concentration of L_1Co complex solution in ethanol at λ = 276nm

Absorbance	Concentration
0.062	2×10^{-5}
0.070	4×10^{-5}
0.135	6×10^{-5}
0.201	8×10^{-5}
0.315	2×10^{-4}
0.549	4×10^{-4}
0.789	6×10^{-4}
1.083	8×10^{-4}
1.119	1×10^{-3}
2.242	2×10^{-3}

Table (2): The absorbance of different concentration of L_2Co complex solution in ethanol at λ = 278nm

Absorbance	Concentration
0.023	1×10^{-5}
0.068	2×10^{-5}
0.135	4×10^{-5}
0.197	6×10^{-5}
0.244	8×10^{-5}
0.311	9×10^{-5}
0.302	1×10^{-4}
0.631	2×10^{-4}
1.001	3×10^{-4}
1.308	4×10^{-4}
1.803	6×10^{-4}
2.476	8×10^{-4}

The plot of the measured absorbance versus the molar concentrations show a straight line obeys Beer's-Lambert law within a concentration ranges(2×10^{-5}–2×10^{-3})M and a determination limit (7.7 – 773.8 μg/ml) with R^2 = 0.9931, RSD = 0.5% for L_1Co Fig (3), and a concentration ranges (1×10^{-5}–8×10^{-4})M and a determination limit (6.9 – 555 μg/ml) with R^2 = 0.9981, RSD = 2.1% for L_2Co Fig.(4).

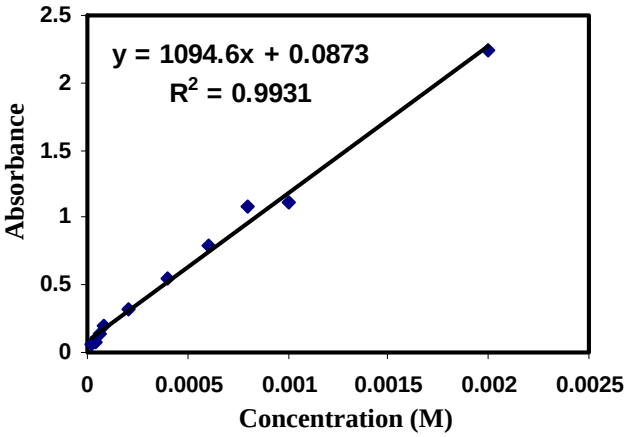

Fig. (3): The zero -order calibration curve of L_1Co complex solution at different concentration at λ = 276 nm

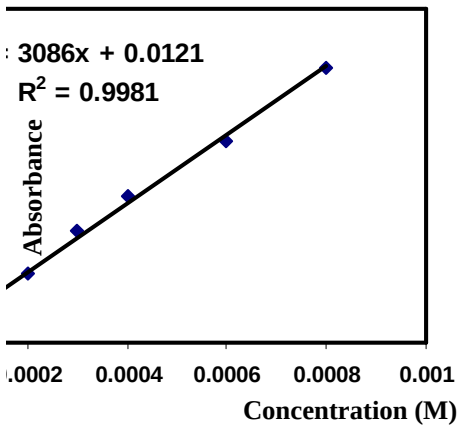

Fig. (4): The zero -order calibration curve of L_2Co complex solution at different concentration at λ = 278 nm

The first order derivative spectra for a series of solutions were recorded and shows for the complex L_1Co a positive band at λ = (208 – 242)nm and crosses the zero axis at λ =242nm, and negative band at λ = (242 – 262)nm and another positive band at λ = (262 – 276)nm and crosses the zero axis at λ = 276nm and another negative peak at λ = (276 – 350)nm. For quantification the integrated area under the negative peak at λ = (242 – 262)nm were recorded for a series of different molar concentrations solution and plotted versus the molar concentration and results in a straight line obeys the Beer's–Lambert law within the concentration range (4×10^{-5}–3×10^{-3})M and a determination range (15.5–1160.8)μg/ml, R^2=0.9913, RSD = 8.8%, table (3), Fig. (5).

Table (3): The integrated area under the peak λ = (242 – 262)nm for different concentration of L_1Co in ethanol

Area	Concentration
0.008	4×10^{-5}
0.027	6×10^{-5}
0.011	8×10^{-5}
0.037	2×10^{-4}
0.141	4×10^{-4}
0.182	6×10^{-4}
0.347	8×10^{-4}
1.180	2×10^{-3}
1.776	3×10^{-3}

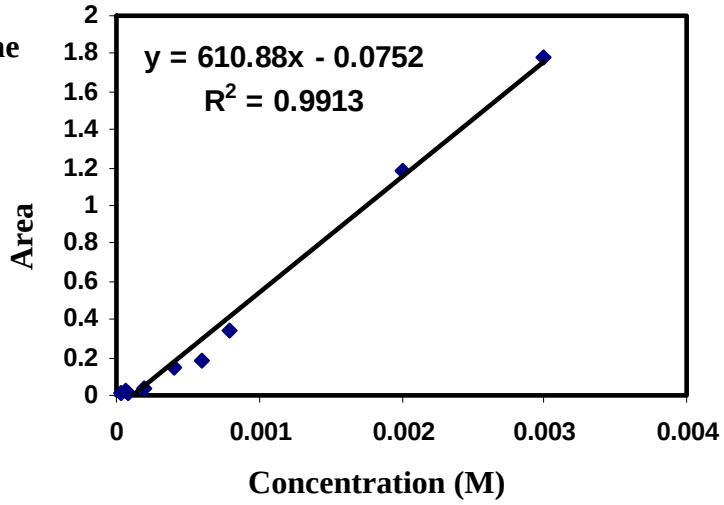

Fig. (5): The calibration curve between the integrated area under the peak measured at different concentration in ethanol at λ = (242 – 262)nm of L_1Co complex solution.

The first order spectrum of the complex L_2Co show a positive band at λ = (212 – 238)nm and crosses the zero axis at λ = 238 nm and a negative band at λ = (238 – 260)nm and another positive band at λ = (260 – 278)nm and crosses the zero axis at λ=278nm and negative band at λ =(278 - 300)nm.

The quantification were accomplished through the plotting of the recorded integrated area under the positive peak at λ = (260 – 278)nm versus the different molar concentration solutions of the complex, the result was a straight line obeys Beer's – Lambert Law within a concentration range (1×10^{-5}–6×10^{-4})M and a determination limit (6.9 – 416.3) μg/ml , R^2 = 0.9913, RSD = 5.3%, table (4), Fig. (6).

Table (4): The integrated area under the peak λ = (260 – 278)nm for different concentration of L_2Co in ethanol

Area	Concentration
0.019	1×10^{-5}
0.026	2×10^{-5}
0.058	6×10^{-5}
0.064	8×10^{-5}
0.066	9×10^{-5}
0.102	1×10^{-4}
0.254	2×10^{-4}
0.453	3×10^{-4}
0.639	4×10^{-4}
0.986	6×10^{-4}

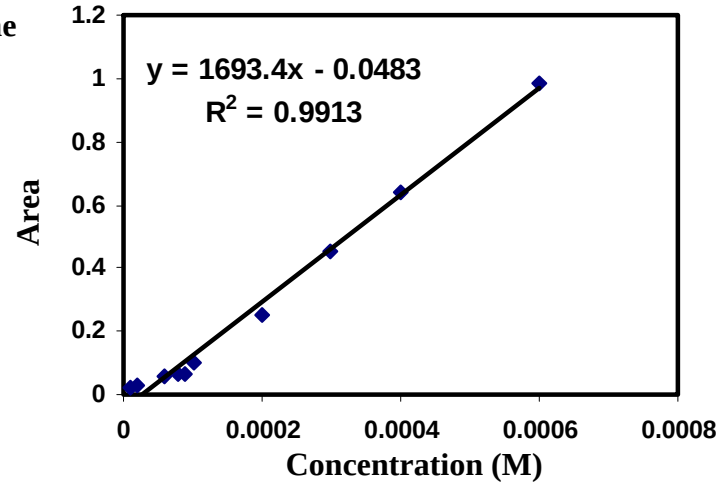

Fig. (6): The calibration curve between the integrated area under the peak measured at different concentration in ethanol at λ = (260 – 278)nm of L_2Co complex solution.

The second order derivative spectrum of the complex L_1Co consists of a negative peak at λ_{max} =242nm and two satellites one on each side of this peak and another negative peak at λ_{max} = 276nm which was selected for the direct quantification of the L_1Co complex in ethanol, which were accomplished by recording the integrated area under this peak for a series of ethanolic solutions of a series of different concentrations of L_1Co , table (5).

On plotting of the integrated area versus the molar concentrations of L_1Co complex the result was a straight line obeys the Beer's-Lambert Law within the concentration range

$(2 \times 10^{-5} - 2 \times 10^{-3})$M , and a determination limit (7.7 – 773.9) μg/ml , R^2 = 0.9963 and RSD (relative standared deviation) = 3.2%, Fig. (7).

Table (5): The integrated area under the peak λ = (276 – 288)nm for different concentration of L_1Co in ethanol

Area	Concentration
0.002	2×10^{-5}
0.003	4×10^{-5}
0.007	6×10^{-5}
0.010	8×10^{-5}
0.016	2×10^{-4}
0.033	4×10^{-4}
0.044	6×10^{-4}
0.064	8×10^{-4}
0.069	1×10^{-3}
0.141	2×10^{-3}

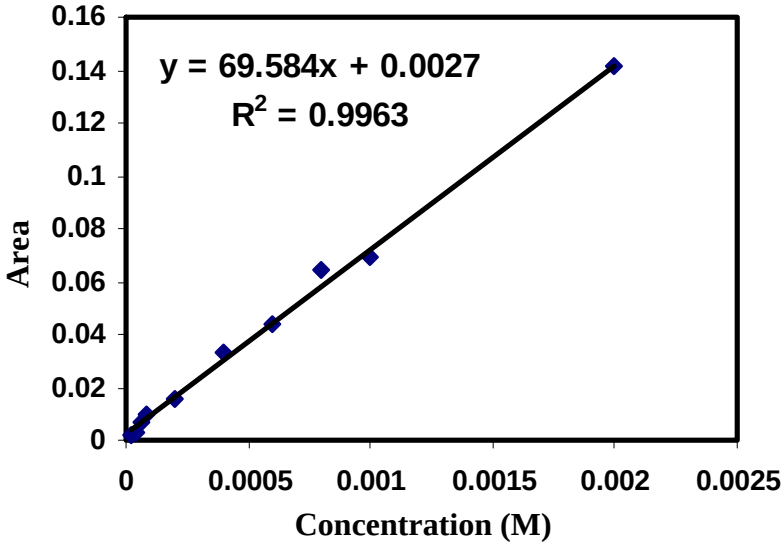

Fig. (7): The calibration curve between the integrated area under the peak measured at different concentration in ethanol at λ = (276 – 288)nm of L_1Co complex solution.

The second order derivative spectrum of L_2Co complex in ethanol show a negative peak at λ_{max} = 238nm and 278nm with two satellites at each side of these peaks.

The direct quantification of the complex L_2Co in ethanol was accomplished by the plot of the recorded integrated area under the negative peak at λ = 278 for a series of different concentrations versus the molar concentrations resulted in a straight line relation obeys the Beer's-Lambert law within a concentration range $(1 \times 10^{-5} - 8 \times 10^{-4})$M and a determination limit (6.9 – 555.0) μg/ml , with R^2 = 0.9930, RSD=2.9%, table (6), Fig. (8).

Table (6): The integrated area under the peak λ = (260 – 286)nm for different concentration of L_2Co in ethanol

Area	Concentration
0.002	1×10^{-5}
0.004	2×10^{-5}
0.010	4×10^{-5}
0.010	6×10^{-5}
0.012	8×10^{-5}
0.013	9×10^{-5}
0.015	1×10^{-4}
0.034	2×10^{-4}
0.056	3×10^{-4}
0.069	4×10^{-4}
0.092	6×10^{-4}
0.137	8×10^{-4}

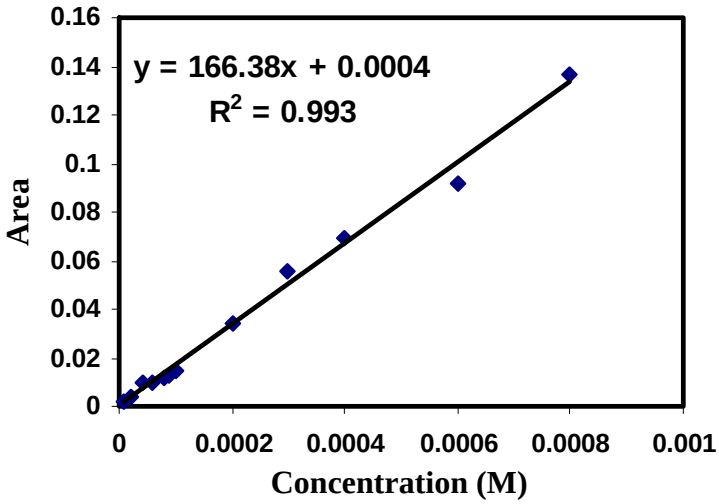

Fig. (8): The calibration curve between the integrated area under the peak measured at different concentration in ethanol at λ = 278nm of L_2Co complex solution.

The results of the direct quantifications of L_1Co shows that the most reliable U.V. spectroscopic technique was the second order derivative > zero order > first order derivative where as for the complex L_2Co, the more reliable technique was the second and the zero order derivative than the first order derivative technique.

Ni-Complexes:

The zero-order derivative spectrum of the complex L_1Ni in ethanol shows a major band at λ = 234nm and another band of lower intensity at λ=274nm, the former band at λ =234nm was selected for the direct quantification of L_1Ni complex, which was accomplished by recording the absorbance of a series of different concentration solutions of the complex L_1Ni in ethanol, table (7), Fig. (9).

Table (7): The absorbance of different concentration of L_1Ni complex solution in ethanol at λ = 234nm

Absorbance	Concentration
0.080	8×10^{-5}
0.084	2×10^{-4}
0.166	4×10^{-4}
0.224	6×10^{-4}
0.257	8×10^{-4}
0.332	1×10^{-3}
0.664	2×10^{-3}
0.921	3×10^{-3}

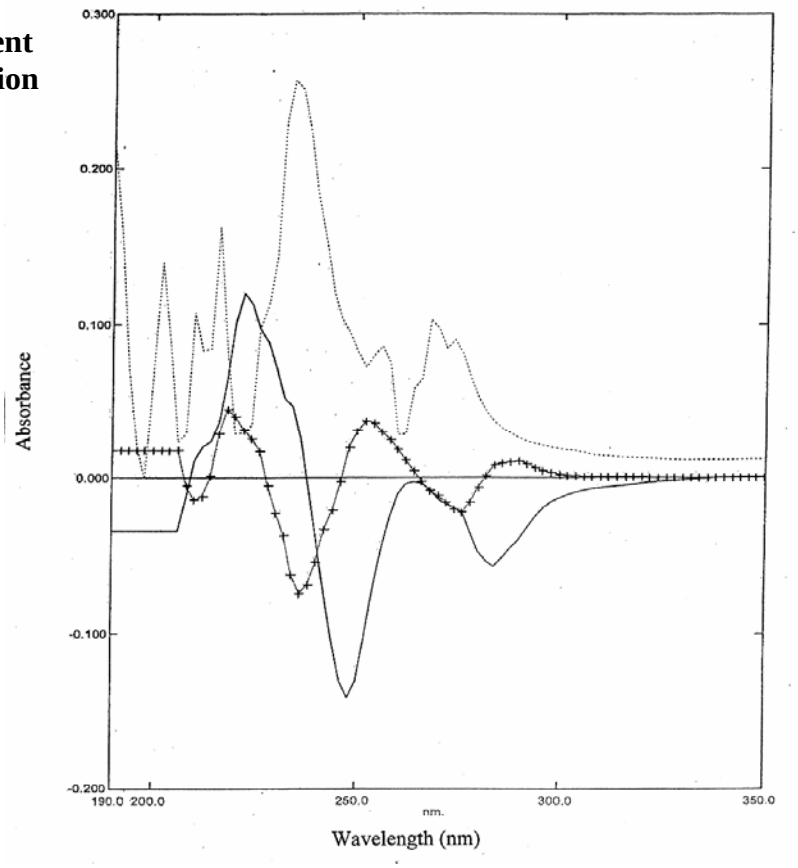

Fig. (9): U.V. absorption spectra of L_1Ni complex solution in ethanol. (…. Zero-order, —— first order derivative , ++++ second order derivative).

The plot of these value results in straight line relation obeys Beer's-Lambert law within the concentration range ($8 \times 10^{-5} - 3 \times 10^{-3}$)M with a determination limit (28.1 – 1052.3) μg/ml , R^2 = 0.9968, RSD = 1.3%, Fig. (10).

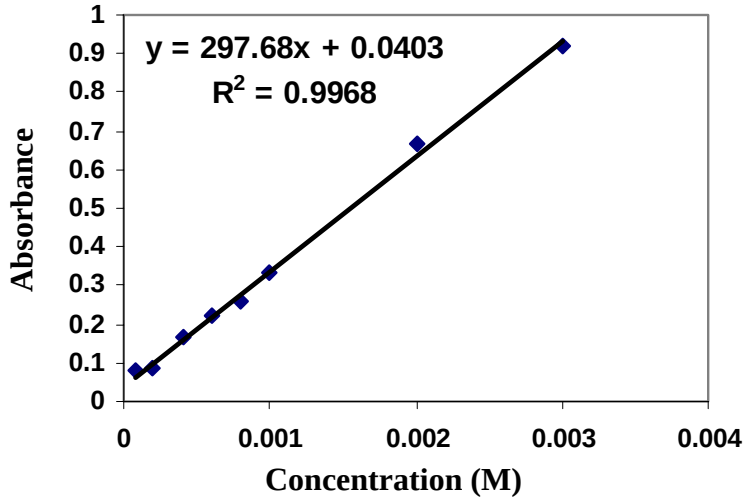

Fig. (10): The zero -order calibration curve of L_1Ni complex solution at different concentration at λ = 234 nm

The zero-order derivative spectrum of L_2Ni complex in ethanol show two absorption bands, the first at λ =240 nm with ε_{max} =1350lit.mole^{-1}.cm^{-1} , and a second broad band at about 290nm. The direct quantification of the complex L_2Ni was accomplished according the absorption band at λ = 240nm, by plotting the recorded absorbance of a series of different molar concentrations, the result was a straight line obeys Beer's-Lambert law within a concentration range ($4 \times 10^{-5} - 3 \times 10^{-3}$)M with a determination limit (14.6 – 1094.0) μg/ml , R^2 = 0.9979, and RSD = 1.4%, Table (8), Fig. (11), Fig.(12).

Table (8): The absorbance of differen concentration of L_2Ni complex solutio in ethanol at λ = 240nm

Absorbance	Concentration
0.054	4×10^{-5}
0.046	6×10^{-5}
0.052	8×10^{-5}
0.102	2×10^{-4}
0.150	3×10^{-4}
0.195	4×10^{-4}
0.286	6×10^{-4}
0.331	7×10^{-4}
0.371	8×10^{-4}
0.445	1×10^{-3}
0.194	3×10^{-3}

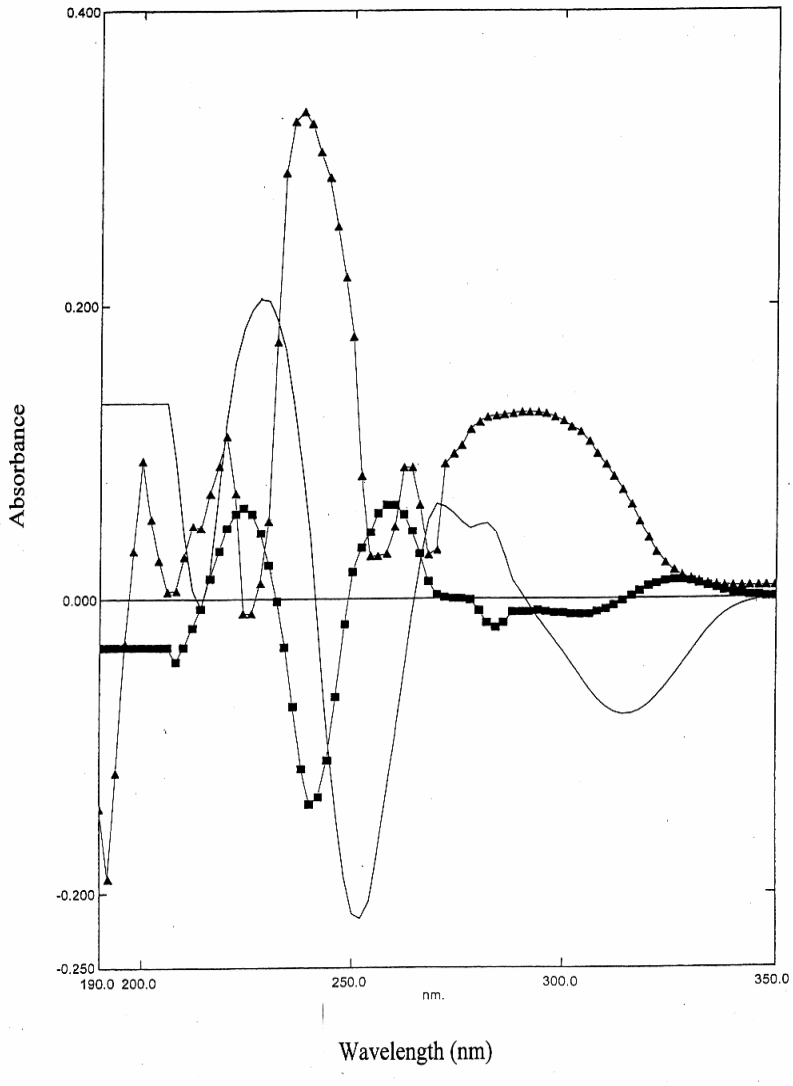

Fig. (11): U.V. absorption spectra of L_2Ni complex solution in ethanol. (▲▲▲Zero-order, —— first order derivative , ■ ■ ■ second order derivative).

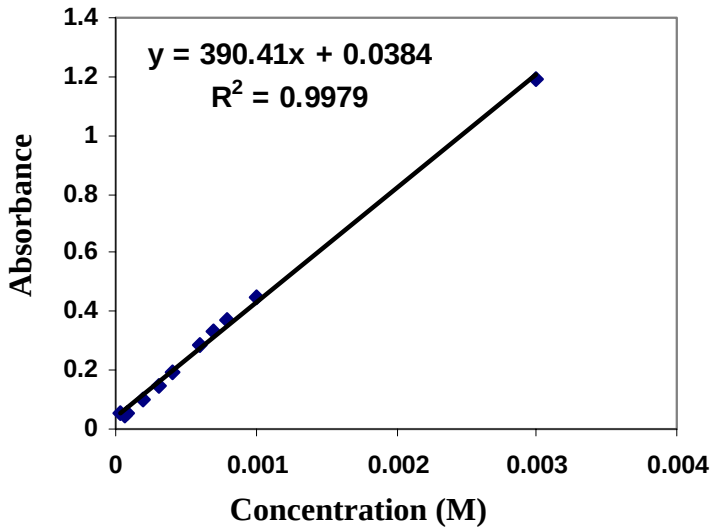

Fig. (12): The zero -order calibration curve of L_2Ni complex solution at different concentration at λ = 240 nm

The first order derivative spectrum of L_1Ni complex solution in ethanol show a positive band at λ = (208 – 236) nm and crosses the zero-axis at λ = 236nm and a negative band at λ = (236 – 264)nm, this band was selected for the direct quantification of L_1Ni complex, the recording of the integrated area under this band for a series of solution of different molar concentrations, and their plots results in a straight line obeys the Beer's-Lambert law within a concentration range ($2 \times 10^{-4} - 5 \times 10^{-3}$)M and a determination limit (70.1 – 1753.5)μg/ml , R^2 = 0.9873, RSD = 12.4%, Table (9), Fig. (13).

Table (9): The integrated area under the peak λ = (236 – 264)nm for different concentration of L_1Ni in ethanol

Area	Concentration
0.006	2×10^{-4}
0.036	4×10^{-4}
0.076	6×10^{-4}
0.088	8×10^{-4}
0.081	1×10^{-3}
0.320	3×10^{-3}
0.458	5×10^{-3}

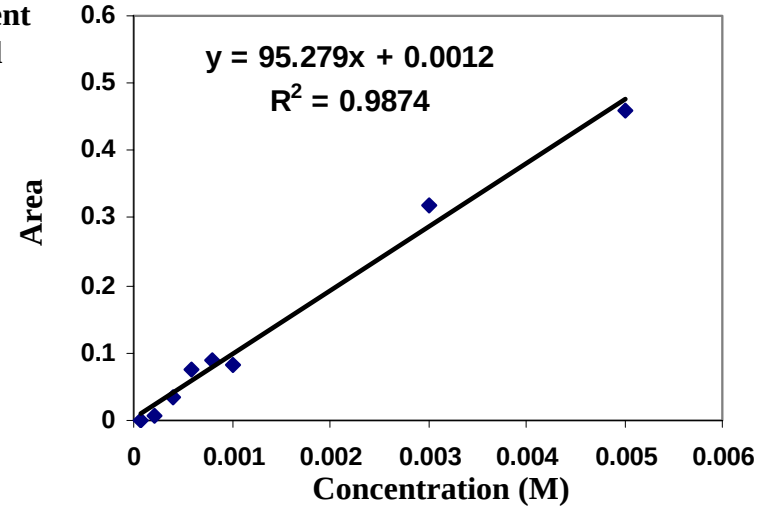

Fig. (13): The calibration curve between the integrated area under the peak measured at different concentration in ethanol at λ = (236 – 264)nm of L_1Ni complex solution.

The first – order derivative spectrum of L_2Ni complex solution in ethanol show a positive peak at λ = (208 – 240) nm and crosses the zero-axis at λ = 240nm and a negative peak at λ = (240 – 266)nm which was taken into consideration for the direct quantification of L_2Ni complex in ethanol by the plot of the recorded of the integrated area under this peak for a series of solution of different concentrations.

The result was a straight line obeys the Beer's – Lambert law within a concentration range (6×10^{-5} – $4 \times$ 10–3)M and a determination limits (21.9 – 1458.8) μg/ml , R^2 = 0.9833, RSD = 9.9%, Table (10), Fig. (14).

Table (10): The integrated area under the peak λ = (240 – 266)nm for different concentration of L_2Ni in ethanol

Area	Concentration
0.049	6×10^{-5}
0.041	8×10^{-5}
0.061	2×10^{-4}
0.121	3×10^{-4}
0.144	6×10^{-4}
0.154	7×10^{-4}
0.187	8×10^{-4}
0.219	1×10^{-3}
0.477	3×10^{-3}
0.560	4×10^{-3}

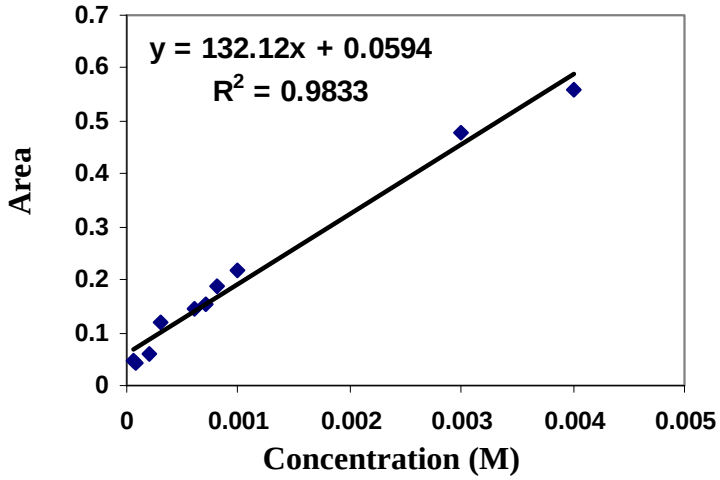

Fig. (14): The calibration curve between the integrated area under the peak measured at different concentration in ethanol at λ = (240 – 266)nm of L_2Ni complex solution.

The second – order derivative spectrum of L_1Ni complex solution in ethanol consists of a main negative peak at λ = (228 – 246)nm and two satellite peaks one at each side of the negative peak.

The quantification of the L_1Ni complex was accomplished through the plot of the recorded integrated area under this peak at λ = (228 – 246)nm for a series of different concentration solutions of L_1Ni in ethanol which result in a straight line obeys Beer's – Lambert law within a concentration range ($8 \times 10^{-5} - 2 \times 10^{-3}$)M and a determination limit (28.1 – 701.4)μg/lm , R^2 = 0.9814, RSD = 10.4%, Table (11), Fig.(15).

Table (11): The integrated area under the peak λ = (228 – 246)nm for different concentration of L_1Ni in ethanol

Area	Concentration
0.001	8×10^{-5}
0.004	2×10^{-4}
0.007	4×10^{-4}
0.010	6×10^{-4}
0.015	8×10^{-4}
0.022	1×10^{-3}
0.053	2×10^{-3}

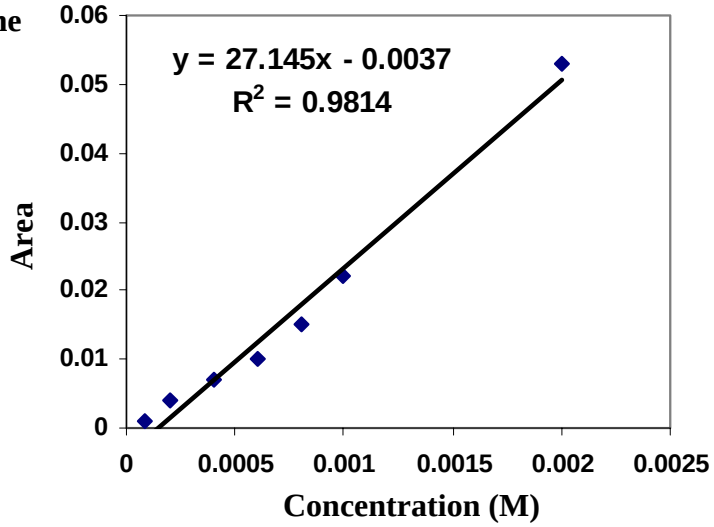

Fig. (15): The calibration curve between the integrated area under the peak measured at different concentration in ethanol at λ = (228 – 246)nm of L_1Ni complex solution.

The second – order derivative spectrum of L_2Ni complex solution in ethanol show a main negative peak at λ = (230 – 250)nm which was taken into consideration for the direct quantification of L_2Ni complex through the plot of the integrated area under the peak versus the molar concentration of L_2Ni complex in ethanol which result in a straight line obeys Beer's – Lambert law within the concentration range $(6\times10^{-5}–3\times10^{-3})$M , and a determination limit (21.9 – 1094.1)µg/ml , R^2 = 0.9938, RSD = 2.3%, Table (12), Fig. (16).

Table (12): The integrated area under the peak λ = (230 – 250)nm for different concentration of L_2Ni in ethanol

Area	Concentration
0.005	6×10^{-5}
0.010	8×10^{-5}
0.019	3×10^{-4}
0.024	6×10^{-4}
0.027	7×10^{-4}
0.031	8×10^{-4}
0.041	1×10^{-3}
0.099	3×10^{-3}

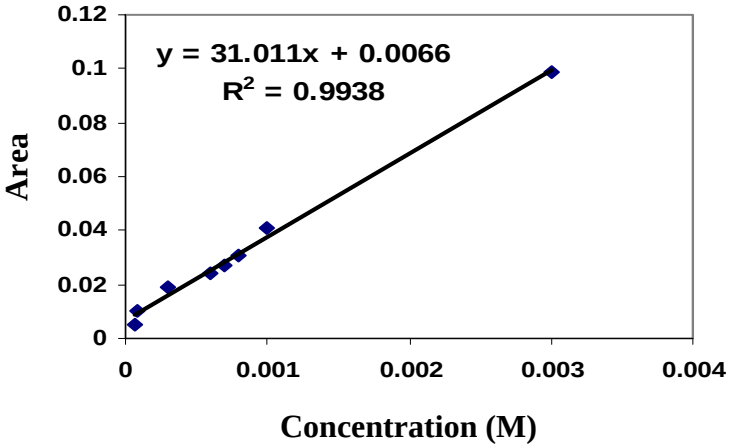

Fig. (16): The calibration curve between the integrated area under the peak measured at different concentration in ethanol at λ = (230 – 250)nm of L_2Ni complex solution.

From the above results were found that the more reliable technique for the direct quantification of:

Complex L_1Ni : zero – order > second
Complex L_2Ni : – order > first order derivative spectra

References:

1. V.S. Shrivastava,C.P.Bhasin,G.C.Saxena, ***J.Indian Chem. Soc***., 1986, **15(2)**, 297.
2. S. Rao, A.S. Mittra, ***J. Indian Chem. Soc***., 1978, **55**, 420.
3. A.K. Mittal, O.P. Singhal, ***J. Indian Chem. Soc***., 1986, **63(67),** 759.
4. S.J. Yan, W.H. Burton, P.L. Chlen, C.C.Cheng, ***J. Heterocycl. Chem.***, 1978, **15(2)**,297.
5. Dash B., Patra M. and Mahapatra P., ***J. Indian chem.* Soc**., 1983, **60**, 772.
6. I.A. Savich, A. K. Pikaev, I.A. Lebedev, V.I. Spitsyn., ***Chem., Abst***., 1334b 1959, **53**, 1-4.
7. Cyba, A. Henryk, ***Chem. Abst***., 68022p, 1968, **69**, 18.
8. Hassaan, M.A. Aly, ***J. Pharm. Sci***., 1992, **33,** (3-4), 679.
9. Sharma, K. Praveen, *Dubey, N.Surendraproc.*, ***Inidan Acad. Sci., Chem. Sci.,*** 1994, **106**, 1,23.
10. S. T. Sulaiman, A.G. Abed, ***Raf. Jour. Sci***., 2002, **13**,1,18.
11. H.A.A. Medien, *Spectrochimica Acta Part A:* ***Molecular and Biomolecular spectroscopy***, 1998, **24(2)**, 359.
12. K. Siddappa, M. Mallikarjum, P.T. Reddy, M.Tambe, ***Ecl. Qnin***.,2008, **33(4)**,41.
13. R.A. Thakur, J.S.Smith, ***J. agric. Food chem.***., 1996, **44(4)**,1047.
14. J. Shah, M.R. Jan, F. Rehman., ***J.Chil. Chem., Soc.***, 2008, **53(3)**,1605.
15. G. Zorana, L. Zvjezdana, K. Natalija, ***Anylist***, 1994, **119(17)**, 1999.
16. G. Zoran, L. Zvjezdana, K. Natalija, ***Talant***, 1994, **4119(25),** 2153.
17. T.Y. Yousif, ***Tikrit Journal of Pure science***, 2009, **14(1)**,1813.
18. N. A. Nawwar, A. M. Shallby, N. M. Hosney and M.M. Mostafa., ***Transition Metal Chemistry***, 2001, **26**, 108.